# Predicting Drug-Efficiency and Cancer Evolution Using an Automated Histological Classification Based on Whole Slide Images

**Yating Pan**
Shanghai University of Traditional Chinese Medicine
**Xinyi Liao**
Shanghai University of Traditional Chinese Medicine
**Xiang Ruan**
The Second Military Medical University
**Yating Deng**
Shanghai University of Traditional Chinese Medicine
**Fan Du**
Shanghai University of Traditional Chinese Medicine
**Guanzhen Yu** ( qiaoshanqian@aliyun.com )
Shanghai University of Traditional Chinese Medicine
**Xiaojun Wu**
Fudan University Shanghai Cancer Center

**Research Article**

**Keywords:**

**Posted Date:** April 1st, 2022

**DOI:** https://doi.org/10.21203/rs.3.rs-1402911/v1

# Abstract

Liver disease is a general term for all diseases that occur in the liver, including cirrhosis, tumors, and drug-induced injury. Liver pathology reveals the pathological appearance of various common liver diseases. Automated classification of liver pathological features based on whole slide images can help observe disease processes and assess drug efficacy, and reduce scientific fraud. Using pathological slides of rat liver induced by the chemical carcinogen TAA, we developed a deep-learning framework to detect abnormal lesions in rat liver from whole histopathological slides. Our framework provides an objective and reproducible method to observe liver lesions and also calculates the proportion of lesions in each liver slide. The framework can also clearly delineate the edges of the liver, revealing whether there are uneven, jagged or wavy surfaces. This tool not only discloses the multi-level pathological evolution of cholangiocarcinoma, but also presents a visual image of the protective effect administered by H2. Artificial intelligence-based algorithms are highly promising methods for studying cancer evolution, assessing drug efficiency, and reducing scientific misconduct.


# Introduction

Scientific progress is based on the establishment of scientific integrity, and academic misconduct has been a stumbling block in the way of scientific career[1]. Among them, image forgery occupies a certain position, and with the development of technology, such as the emergence of powerful functions of Photoshop, ImageJ and other graphics software, while providing convenience for researchers, it is also abused by some authors who try to manipulate images, making the means of image forgery more technical and covert[2]. In the face of such a critical situation, it is urgent and important to prevent image fraud, which requires enriching techniques for deep image verification. The easiest way to solve this problem is to make the work of researchers accessible to non-specialists. For example, when evaluating liver disease, researchers should provide slides of the entire liver, rather than partial zooms of selected areas, and use technology to show all lesion slides of the entire liver, so that reviewers, editors, and even laypeople can understand the presence of lesions and the effectiveness of treatment. Here, artificial intelligence (AI) technology is one such technological tool.

Artificial intelligence (AI) is a technology that enables computer to mimic human intelligence. The explosion of machine learning, especially deep learning, has led to a shift in the way we live our daily lives[3]. Among other things, in the field of medicine, AI has enormous potential, whether in supporting clinical diagnosis, patient management or treatment planning[4]. Given the sheer volume that characterizes medical data itself, it provides room for continuous advancement in deep learning. It is currently excelling in driving various imaging-related fields, including but not limited to radiology[5], oncology[6] and digital pathology[7].

Nowadays, AI has been able to automatically detect tumor tissues, thus reducing the workload of pathologists[8]. In addition, AI may be able to capture more of the histological features in predicting tumor

staging than pathologists, and this is particularly noticeable in gastrointestinal and liver tumors[9]. Studies have shown that tumor-infiltrating lymphocytes are closely related to the prognosis of gastric cancer patients, and tumor-infiltrating lymphocytes on pathological tissues can be detected by Convolutional Neural Network (CNN) models, thus providing a good predictive prospect for tumor prognosis[10]. In hepatocellular carcinoma (HCC), AI models can predict survival after tumor resection more accurately than a multifaceted composite total score[11].In particular, AI has been shown to infer molecular and genetic changes in cancer tissues from histological digital sections[9]. This indicates that the application of artificial intelligence in pathology provides a good environment for the development of precision treatment of digestive system tumors.

Liver lesions reflect changes in the function and metabolism of the organism caused by external stimuli or its own diseases[12]. By observing morphological and pathological changes in the liver, we can grasp the onset and progression of various diseases and the body's response to drug efficacy and toxicity. Liver lesions in animal models mainly include inflammatory diseases[13], metabolic diseases[14], and proliferative diseases[15]. In previous studies, we established that thioacetamide(TAA)-induced abnormal proliferation of intrahepatic bile duct epithelium leads to bile duct intraepithelial neoplasia, which is a precancerous from of bile duct cancer[16]. We have used this model to intervene with aspirin, herbs, and hydrogen-rich water with positive results. In the experiment with hydrogen-rich water intervention[17],our algorithmic model clearly shows the location and amount of liver fibrosis, visualizes the differences between the two treatment options, and provides objective quantitative indicators. However, there are two other main features of this animal model that this algorithm does not address: one is the surface state of the liver and the other is the difference between fibrosis and neoplasia.

For these animal liver models, we have developed a new deep learning network for liver disease segmentation to identify different pathological features of liver lesions, with the aid of artificial intelligence to visualize the lesion sites and quantify the results more intuitively.

# Methods

1. **Pathology data sets**

The data used in this study were pathological liver slides from rats. A total of 56 slides were used for fibrosis and tumor identification, including 23 TAA pathological liver slides, 22 TAA+H2 pathological liver slides, and 11 normal liver pathological slides. Due to the high resolution of the original pathology section images, it tends to cause the problem of insufficient computer memory. Therefore, the original images must be cut into smaller patch images. In this regard, we cut each original image and its labeled image into 100 patch images with a resolution of 768 × 768 to obtain a total of 5600 images, of which 4200 images were randomly selected as the training set and the remaining 1400 as the validation set, as shown in Figure 1.

2. **Contour Detection**

In the liver contour detection part, the images of animal pathological liver contours were extracted in this study. Specifically, for the original image of pathology, the K-Means algorithm was used to segment the region of interest in the image, and then the convex hull was removed and the hole was filled, and the liver edge contour in the form of edges was extracted, as shown in Figure 2A.

3. **Identification of tissue fibrosis**

Based on the liver contour extraction, the tissue fibrosis was further identified, and the whole process is shown in Figure 2B. The dataset was trained, and the images were annotated with fibrosis by ASAP data annotation software to obtain the corresponding annotated images. In order to improve the extraction accuracy of tissue fibrosis, the regions with tissue fibrosis are mainly clipped when cutting the patch images.

In view of the good performance of U-NET in medical image segmentation, this study uses U-NET model for end-to-end training of cropped pathological images. Before training, MODEL cuts ROIs from the original images based on the fibered segmentation mask, resizes them to 256*256, and normalizes them. The U-NET model used in this study has cross entropy as the loss function, a learning rate of 0.0001, a maximum iteration step size of 100, and a downsampling rate set to 0.5. The Adam optimizer is used to update the model parameters. To increase the diversity of the data and to avoid overfitting the model, incremental processing of the data, such as rotation and mirroring, was performed before training. During testing, the retained model was used to identify tissue fibrosis in the original images to obtain the proportion of tissue fibrosis.

4. **Tumor Identification**

Based on the identification of tissue fibrosis, the tumor was further identified and the whole process is shown in Figure 2C. Similarly, the dataset was trained and the images were labeled with tumors by ASAP data labeling software to obtain the corresponding labeled images. Due to the small amount of tumor data, the patch images were cropped to focus on the tumor region in order to improve the extraction accuracy.

In this study, theNeural Conditional Random Field (NCRF) deep learningalgorithm proposed by Baidu Research Institute is used to train cropped pathology images[18].The NCRF algorithm inputs more than one image, but cuts the image into a grid, along with the feature extractors around the image, to the CNN, which encodes the feature extractors of each image block into a fixed vector representation, while using neural conditions to airport modeling of the spatial relationships in the image to predict whether it is a tumor cell or not. The entire algorithm can be trained end-to-end on the GPU without any post-processing. During testing, the retained model is used to identify the tumor in the original image and obtain the tumor proportion.

# Results

Pathological image recognition of animal liver lesions is mainly divided into three parts: liver contour detection, tissue fibrosis recognition and tumor recognition.The overall framework is shown in Figure 1.

1. **TAA lesion liver**

The TAA lesions were divided into 8, 12, 16 and 20-week groups according to the lesion cycles. Figure 3A shows the recognition results of different cycles.In order to intuitively understand the influence of lesion cycle on the lesion liver, we counted the proportion of fibrosis, the proportion of tumor and the number of tumor in pathological sections of TAA lesion liver with different lesion cycles, and took their average value, as shown in Figure 3B, C, D.Among them, the mean proportions of liver fibrosis in TAA lesions at 8, 12, 16 and 20 weeks were 2.05±0.11, 7.29±5.80, 29.2±11.54 and 31.44±8.03, the mean proportions of tumor were 0±0, 0.01±0.02, 1.83±1.21 and 3.93±2.09, and the mean numbers of tumor were 0±0, 0.25±0.43, 5.25±2.68 and 4±2.05, respectively.This suggests that the proportion of fibrosis and tumors in the TAA lesioned liver increases with the duration of the lesion.

2. **TAA+$H_2$ lesions in liver**

The TAA+$H_2$ lesions were also divided into 8, 12, 16 and 20-week groups according to the lesion cycle. Figure 4A shows the recognition results of different cycles.Just like TAA diseased liver, in order to intuitively understand the influence of lesion cycle on the diseased liver, we counted the proportion of fibrosis, the proportion of tumor and the number of tumor in pathological sections of TAA+$H_2$ diseased liver with different lesion cycles, and took their average value, as shown in Figure 4B, C, D.Among them, the mean proportions of liver fibrosis in TAA lesions at 8, 12, 16 and 20 weeks were 2.35±0.88, 2.29±0.67, 20.07±16.51and 14.75±16.14, the mean proportions of tumor were 0±0, 0±0, 0.89±0.95 and 2.44±4.04, and the mean numbers of tumor were 0±0, 0±0, 0.75±0.83 and 1.36±2.14, respectively. This suggests that the proportion of fibrosis and tumors in the TAA+H2 lesioned liver increases as the duration of the lesion increases.

3. **Comparison of TAA and TAA+$H_2$ lesions in liver**

In order to verify the effect of $H_2$ on the liver with TAA lesions, the proportion of fibrosis, the proportion of tumor and the number of tumors were compared between TAA and TAA+$H_2$ lesions. As can be seen from Figure 5, the fibrosis of the liver with TAA+$H_2$ lesions is significantly less than that of the liver with TAA lesions, and there is no tumor area.The comparative statistical figure is shown in Figure 5B, C, D. the proportion of fibrosis, the proportion of tumor and the number of tumor in the liver with TAA+$H_2$ lesions were all lower than that in the liver with TAA lesions in different cycles.The above results verified that $H_2$ has a good effect on TAA lesion liver.

# Discussions

1. Innovative discoveries

Our study provides strong evidence that a deep learning framework is useful for detecting abnormal lesions in rat liver from whole histopathology slices. The high performance of our framework not only provides an objective and reproducible method to visualize liver lesions, but also calculates the proportion of lesions in the whole liver slice. Interestingly, our framework can clearly outline the edges of the liver, showing if there are uneven, jagged or wavy surfaces. In addition, proliferative lesions that are different from biliary fibrosis are also correctly detected by our frame, which is then calculated and numbered.

2. WSI Study of disease evolution

Cancer develops through a multi-step process of somatic cell evolution accompanied by a multi-step morphological continuum of transformation from normal cells to preneoplastic to benign and then to malignant tumors. Mutagenic forces lead to a time-scale accumulation of point mutations throughout the cancer transformation process, observed in the progressively deteriorating morphology of healthy tissue[19]. All these morphological pathological changes[20], together with specific driver mutations[21], can be identified and extracted by machine learning methods. Not surprisingly, automated histopathological analysis depends on image features including cell size, shape, distribution of pixel intensities, texture of cells and nuclei, and tumor microenvironment[20]. The multi-step process of CCA would go through normal bile duct to biliary dysplasia to infiltrative CCA, which can be pathologically reproduced by a rat model of thioacetamide-induced[22]. The most important pathological changes include wavy rims in the liver, bile duct hyperplasia and CCA with intense stromal demyelination (the latter is known as gallbladder fibrosis), whose image features are extracted with biological significance. We built an automated pipeline to identify these three objective features based on image labels annotated by trained pathologists. Our machine learning model clearly shows the contours of the liver, identifies the diffusely distributed liver lesions in WSIs, and classifies CCA from all lesions. Notably, our classifier can systematically document the histopathological evolution of TAA-induced biliary tract disease in rats.

3. Study of therapeutic effects and adverse effects of drugs

Machine learning techniques have proven useful in predicting drug response and synergism[23]and adverse drug reactions[24]. For example, researchers have used cellular isolation methods to reflect the extent of drug effects on cells based on the cellular characteristics of cyclic drug administration[25], and other groups have developed an automated machine learning (AutoML) model to classify patterns of drug-induced liver injury over whole slide images[26].·We previously developed an automated lesion detection framework to detect liver lesions from whole slide images (WSIs), defined as Alesion. this AI algorithm can observe the location and number of liver lesions in WSIs, clearly showing the treatment effect of H2 compared to controls[27]. A limitation of this AI algorithm is that it does not distinguish between the different pathological steps of biliary dysplasia and infiltrative CCA. In this study, we selected two additional informative features, namely wavy edges and cholangiofifibrosis, and optimized our classifier. After training and testing images with or without H2 treatment, our machine learning model showed that the total Alesion, number and area of cholangiofifibrosis (originally called CCA) were

effectively reduced by long-term treatment with H2. Our results also show that the model can be used to assess the protective effect of hydrogen-rich saline on liver injury in another animal model[28],as shown inSupplementary Figure1.

4. Reduced falsification

Scientific misconduct or research fraud is a global problem in health-related research. These misconducts can be classified into four categories: overall concern, textual concern, image concern and data concern[29]. However, the tools to investigate all of these research misconducts are rudimentary and labor-intensive[29]. One of the four types of research misconduct is pathological image misconduct. In previous studies, pathology results were presented as small slices of specific magnifications of HE or IHC rather than WSIs of organs or tumor tissue.Fraudulent behavior can occur in this process, including selecting only areas of interest and ignoring areas without lesions, or even taking representative photographs from different parts of the same sample. Automated tools are needed to address these rising challenges. The best way to do this is to present all lesions in WSIs in a way that can be easily understood by laypeople. Despite the visualization and quantification of liver lesions in Supplementary Figure 1, it is still difficult to distinguish whether these images are from different samples or from the same sample. Therefore, an artificial intelligence-based automatic classifier for WSIs would be an effective way to avoid this type of scientific misconduct or research fraud.

# Conclude

In the above paragraphs, we present a fully automated WSI-based deep learning framework to evaluate liver lesions or treatment effects. The model can effectively reflect the three manifestations of chemical carcinogen-induced liver lesions. Thus, we provide a promising tool for future assessment of therapeutic efficacy, toxicity and tumor evolution in animals.

# Abbreviations

AI: Artificial intelligence

CNN: Convolutional Neural Network

HCC: Hepatocellular carcinoma

TAA: Thioacetamide

NCRF: Neural Conditional Random Field

AutoML: Automated machine learning

WSIs: Whole slide images

CCA: Cholangiofifibrosis

# Declarations

**Ethics approval and consent to participate:** No Applicable.

**Consent for publication:** No Applicable.

**Availability of data and materials:** The datasets used and analyzed during the current study are available from the corresponding author on reasonable request.

**Competing interests:** The authors declare no conflict of interest.

**Funding:** This research was supported by the projects from National Natural Science Foundation of China (No.81972721).

**Authors' contributions:** Guanzhen Yu and Xiaojun Wu carried out conception/design; Yating Pan, Xinyi Liao, Yating Deng and Xiang Ruan participated in the acquisition of data; Yating Pan, Fan Du and Xiang Ruan analyzed data and performed interpretation; Guanzhen Yu andXiaojun Wu provided source; Guanzhen Yu wrote the manuscript; Guanzhen Yu and Xiaojun Wu approvedthe final manuscript.

**Acknowledgements:** No further acknowledgements beyond declarations are listed above.

# References

1. Zietman AL. Falsification, Fabrication, and Plagiarism: The Unholy Trinity of Scientific Writing. Int J Radiat Oncol Biol Phys 2013;87(2):225-227. DOI: 10.1016/j.ijrobp.2013.07.004.
2. Castillo Camacho I, Wang K. A Comprehensive Review of Deep-Learning-Based Methods for Image Forensics. JImaging 2021;7(4):69. DOI: 10.3390/jimaging7040069.
3. Huo Y, Deng R, Liu Q, Fogo AB, Yang H. AI applications in renal pathology. Kidney Int 2021;99(6):1309-1320. DOI: 10.1016/j.kint.2021.01.015.
4. Esteva A, Robicquet A, Ramsundar B, et al. A guide to deep learning in healthcare. Nat Med 2019;25(1):24-29. DOI: 10.1038/s41591-018-0316-z.
5. Hosny A, Parmar C, Quackenbush J, Schwartz LH, Aerts HJWL. Artificial intelligence in radiology. Nat Rev Cancer 2018;18(8):500-510. DOI: 10.1038/s41568-018-0016-5.
6. Londhe VY, Bhasin B. Artificial intelligence and its potential in oncology. Drug Discov Today 2019;24(1):228-232. DOI: 10.1016/j.drudis.2018.10.005.
7. Niazi MKK, Parwani AV, Gurcan MN. Digital pathology and artificial intelligence. Lancet Oncol 2019;20(5):e253-e261. DOI: 10.1016/S1470-2045(19)30154-8.
8. Jiang Y, Yang M, Wang S, Li X, Sun Y. Emerging role of deep learning-based artificial intelligence in tumor pathology. Cancer Commun 2020;40(4):154-166. DOI: 10.1002/cac2.12012.

9. Calderaro J, Kather JN. Artificial intelligence-based pathology for gastrointestinal and hepatobiliary cancers. Gut 2021;70(6):1183-1193. DOI: 10.1136/gutjnl-2020-322880.
10. Garcia E, Hermoza R, Castanon CB, Cano L, Castanneda C. Automatic Lymphocyte Detection on Gastric Cancer IHC Images Using Deep Learning. IEEE International Symposium on Computer-based Medical Systems: IEEE; 2017.
11. Saillard C, Schmauch B, Laifa O, et al. Predicting Survival After Hepatocellular Carcinoma Resection Using Deep Learning on Histological Slides. Hepatology 2020;72(6):2000-2013. DOI: 10.1002/hep.31207.
12. Inamine T, Schnabl B. Immunoglobulin A and liver diseases. J Gastroenterol 2018;53(6):691-700. DOI: 10.1007/s00535-017-1400-8.
13. Köhn-Gaone J, Dwyer BJ, Grzelak CA, et al. Divergent Inflammatory, Fibrogenic, and Liver Progenitor Cell Dynamics in Two Common Mouse Models of Chronic Liver Injury. Am J Pathol 2016;186(7):1762-1774. DOI: 10.1016/j.ajpath.2016.03.005.
14. Buyco DG, Martin J, Jeon S, Hooks R, Lin C, Carr R. Experimental models of metabolic and alcoholic fatty liver disease. World J Gastroenterol 2021;27(1):1-18. DOI: 10.3748/wjg.v27.i1.1.
15. Qiu R, Murata S, Cheng C, et al. A Novel Orthotopic Liver Cancer Model for Creating a Human-like Tumor Microenvironment. Cancers 2021;13(16):3997. DOI: 10.3390/cancers13163997.
16. Sibulesky L, Nguyen J, Patel T. Preneoplastic conditions underlying bile duct cancer. Langenbecks Arch Surg 2012;397(6):861-867. DOI: 10.1007/s00423-012-0943-7.
17. Chaofu LI, Gao Y, Zhou Z, et al. Synergistic effect of hydrogen-rich water and Jinfukang oral liquid in prevention of cholangiocarcinoma in rats induced by thioacetamide. Academic Journal of Chinese PLA Medical School 2019.
18. Li Y, Ping W. Cancer Metastasis Detection With Neural Conditional Random Field. arXivcsCV 2018. DOI: arxiv-1806.07064.
19. Gerstung M, Jolly C, Leshchiner I, et al. The evolutionary history of 2,658 cancers. Nature 2020;578(7793):122-128. DOI: 10.1038/s41586-019-1907-7.
20. Yu K-H, Zhang C, Berry GJ, et al. Predicting non-small cell lung cancer prognosis by fully automated microscopic pathology image features. Nat Commun 2016;7(1):12474. DOI: 10.1038/ncomms12474.
21. Coudray N, Ocampo PS, Sakellaropoulos T, et al. Classification and mutation prediction from non–small cell lung cancer histopathology images using deep learning. Nat Med 2018;24(10):1559-1567. DOI: 10.1038/s41591-018-0177-5.
22. Yeh C-N, Maitra A, Lee K-F, Jan Y-Y, Chen M-F. Thioacetamide-induced intestinal-type cholangiocarcinoma in rat: an animal model recapitulating the multi-stage progression of human cholangiocarcinoma. Carcinogenesis 2004;25(4):631-636. DOI: 10.1093/carcin/bgh037.
23. Kuenzi BM, Park J, Fong SH, et al. Predicting Drug Response and Synergy Using a Deep Learning Model of Human Cancer Cells. Cancer Cell 2020;38(5):672-684.e6. DOI: 10.1016/j.ccell.2020.09.014.

24. Raja K, Patrick M, Elder JT, Tsoi LC. Machine learning workflow to enhance predictions of Adverse Drug Reactions (ADRs) through drug-gene interactions: application to drugs for cutaneous diseases. Sci Rep 2017;7(1):3690. DOI: 10.1038/s41598-017-03914-3.
25. Mudali D, Jeevanandam J, Danquah MK. Probing the characteristics and biofunctional effects of disease-affected cells and drug response via machine learning applications. Crit Rev Biotechnol 2020;40(7):951-977. DOI: 10.1080/07388551.2020.1789062.
26. Puri M. Automated Machine Learning Diagnostic Support System as a Computational Biomarker for Detecting Drug-Induced Liver Injury Patterns in Whole Slide Liver Pathology Images. Assay Drug Dev Technol 2020;18(1):1-10. DOI: 10.1089/adt.2019.919.
27. Li C, Zhao X, Gu X, Chen Y, Yu G. The Preventive Role of Hydrogen-Rich Water in Thioacetamide-Induced Cholangiofibrosis in Rat Assessed by Automated Histological Classification. Front Pharmacol 2021;12:1708. (Original Research). DOI: 10.3389/fphar.2021.632045.
28. Sun H, Chen L, Zhou W, et al. The protective role of hydrogen-rich saline in experimental liver injury in mice. J Hepatol 2011;54(3):471-480. DOI: 10.1016/j.jhep.2010.08.011.
29. Bordewijk EM, Li W, van Eekelen R, et al. Methods to assess research misconduct in health-related research: A scoping review. J Clin Epidemiol 2021;136:189-202. DOI: 10.1016/j.jclinepi.2021.05.012.

# Figures

A

| | Numbers of LIver | Training | Test |
|---|---|---|---|
| Livers of TAA-induced rats | 23 | 1700 | 600 |
| Livers of TAA-induced rats affter treated | 22 | 1700 | 600 |
| Normal livers | 11 | 800 | 200 |
| Total | 56 | 4200 | 1400 |

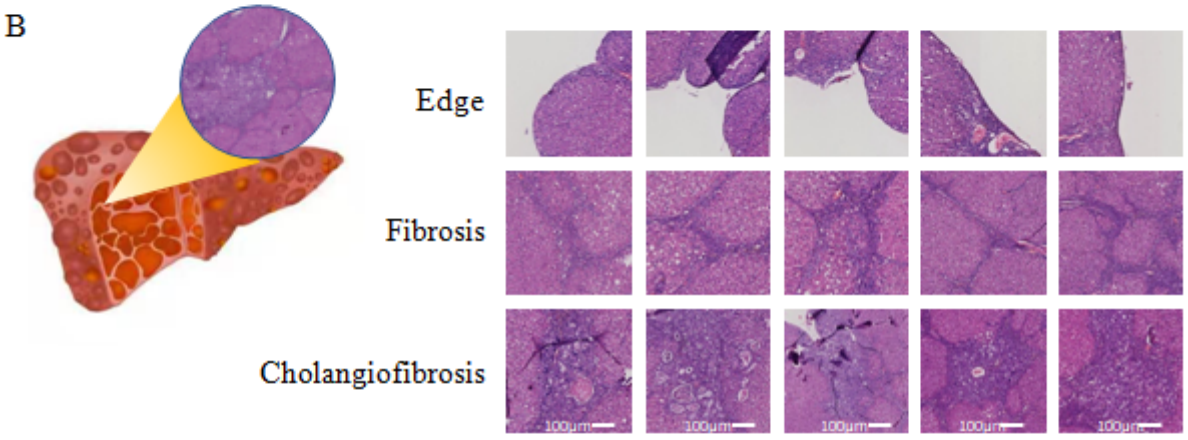


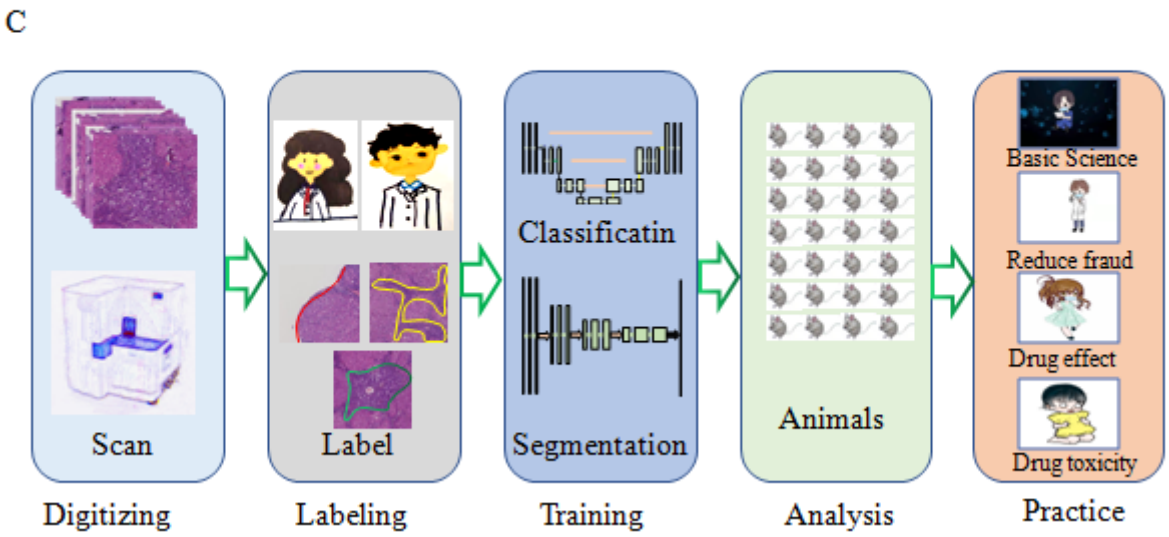


## Figure 1

**Pathology dataset and deep learning network analysis flow chart for liver disease segmentation.**

A. Pathology dataset used in this model.The training set was composed of 4200 WSIs and the test set was composed of 1400 WSIs. B. The main recognition of this model, including liver edge, liver fibrosis and Cholangiofibrosis regions. C. The flowchart of the entire operational analysis of this model. There are five steps including digital scanning of pathological slides, manual labeling, classification and cutting of training model, result analysis, and testing practice.

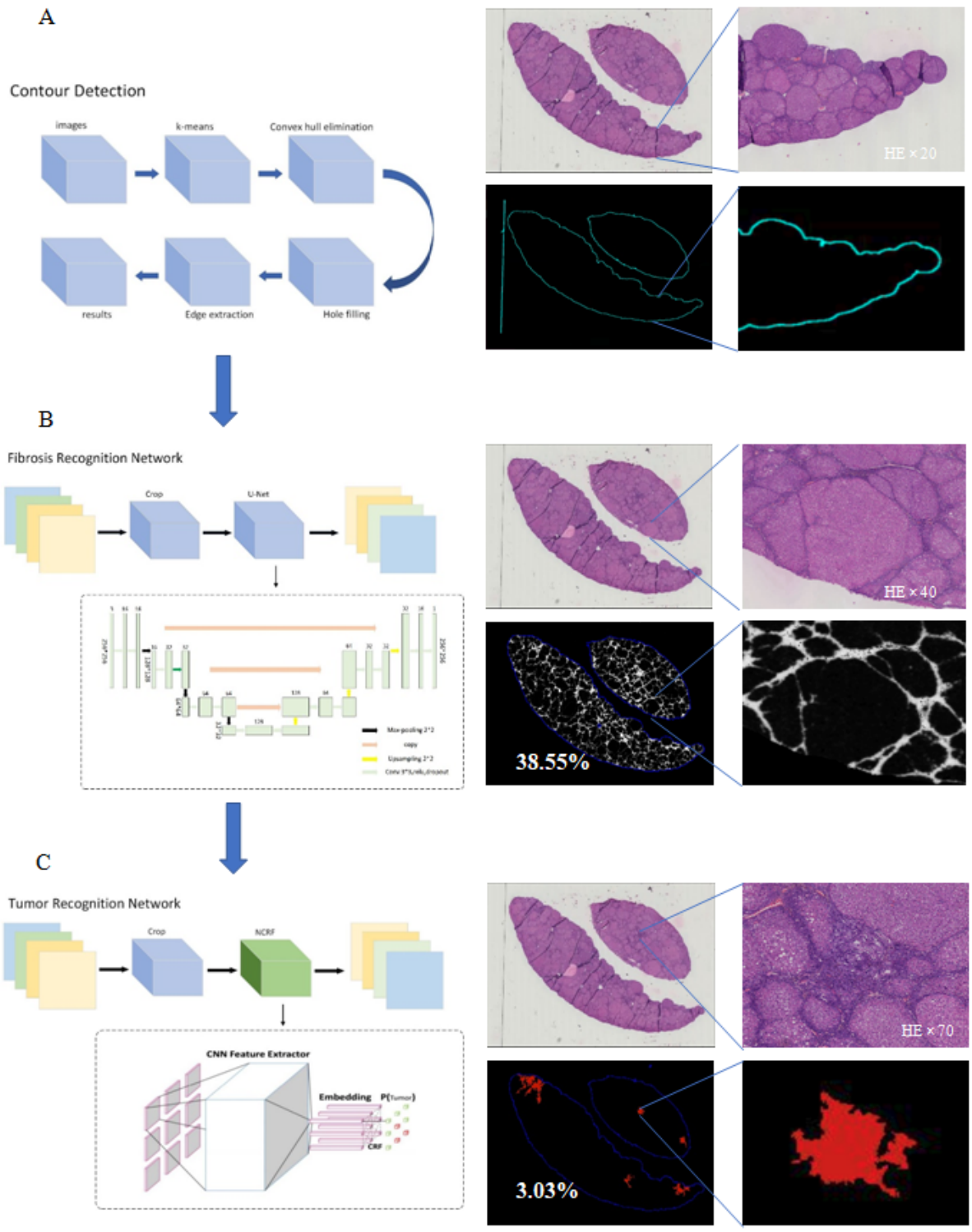


## Figure 2

### Model for training to identify liver lesions.

A. Liver edge detection, the blue part is the identified liver edge. B. Liver fibrosis recognition network, the white part is the identified fibrosis area. C. Liver tumor recognition network, the red part is the identified tumor area.

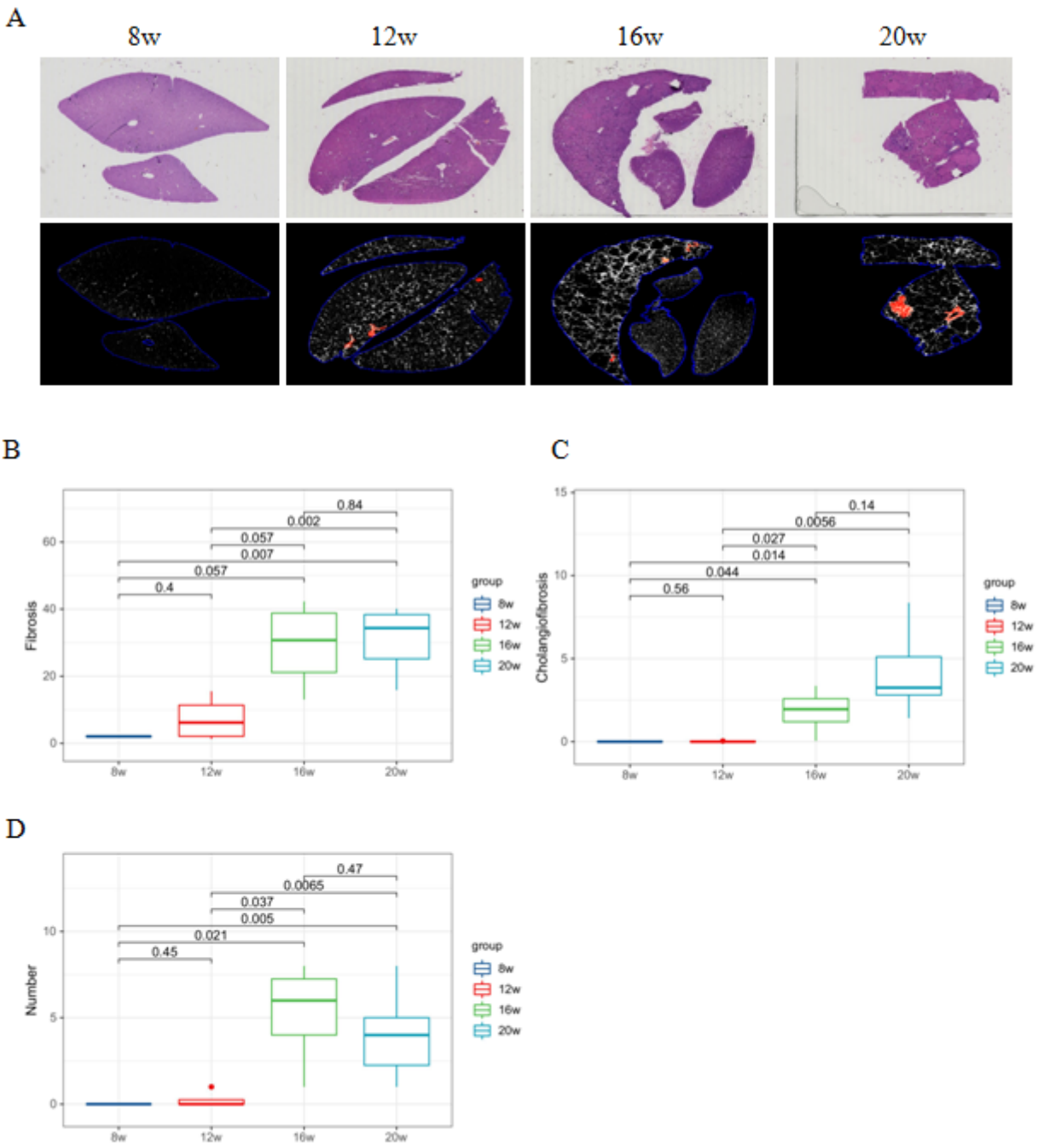


## Figure 3

**AI identification of TAA-induced liver lesions and quantitative analysis.**

A. AI identification of TAA-induced liver tissue lesions in rats under different cycle effects. B. Percentage of liver fibrosis. C. Percentage of bile duct fibrosis. D. Number of liver tumors. T-test was used to determine statistical significance. * $p < 0.05$.

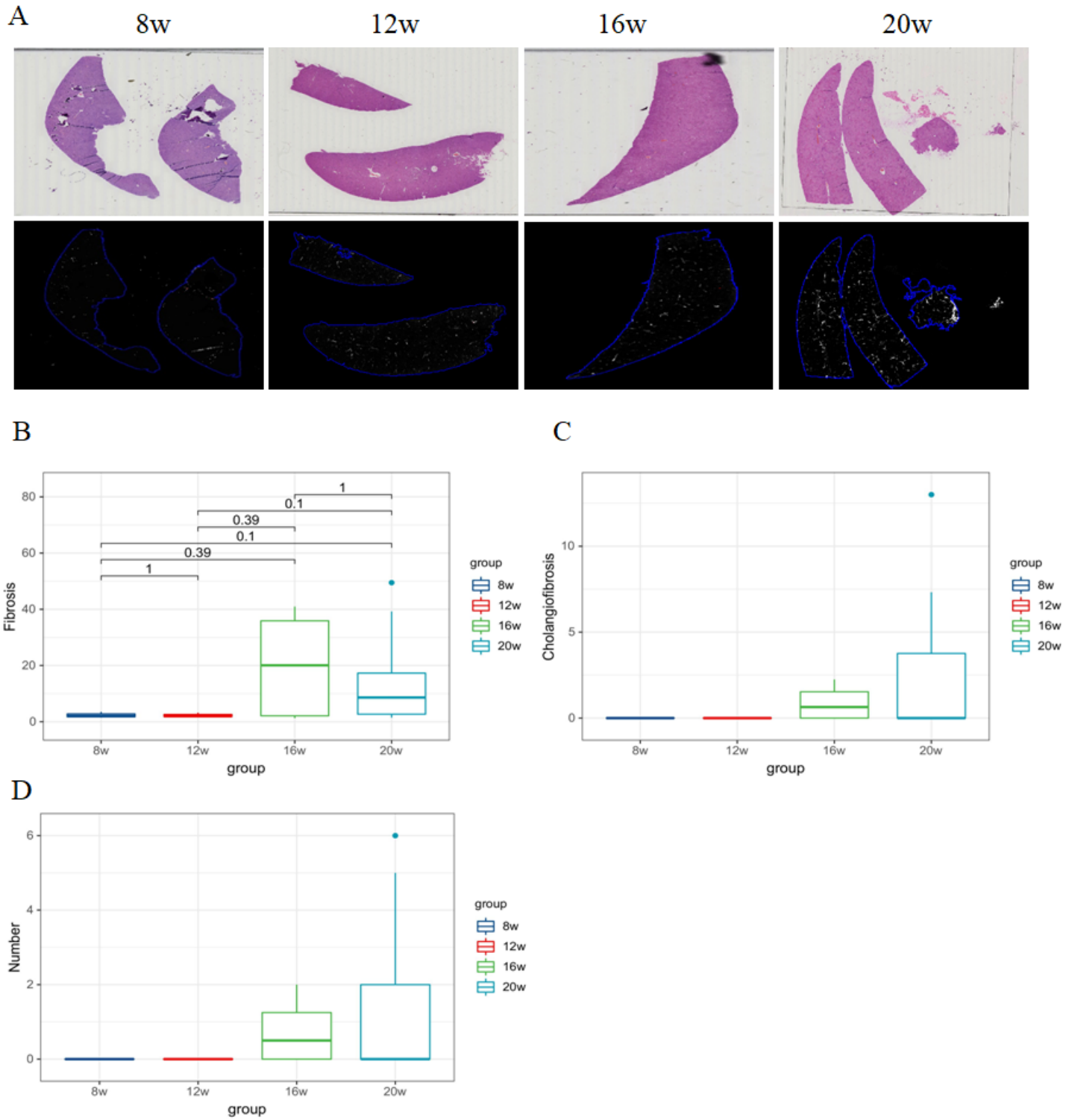


## Figure 4

**AI identification of liver lesions after TAA+H2 intervention and quantitative analysis.**

A. AI identification of liver histopathology in rats after different cycle effects of TAA+H2 treatment. B. Percentage of liver fibrosis. C. Percentage of cholangiofibrosis. D. The number of liver tumors. T-test was used to determine statistical significance. * $p < 0.05$.

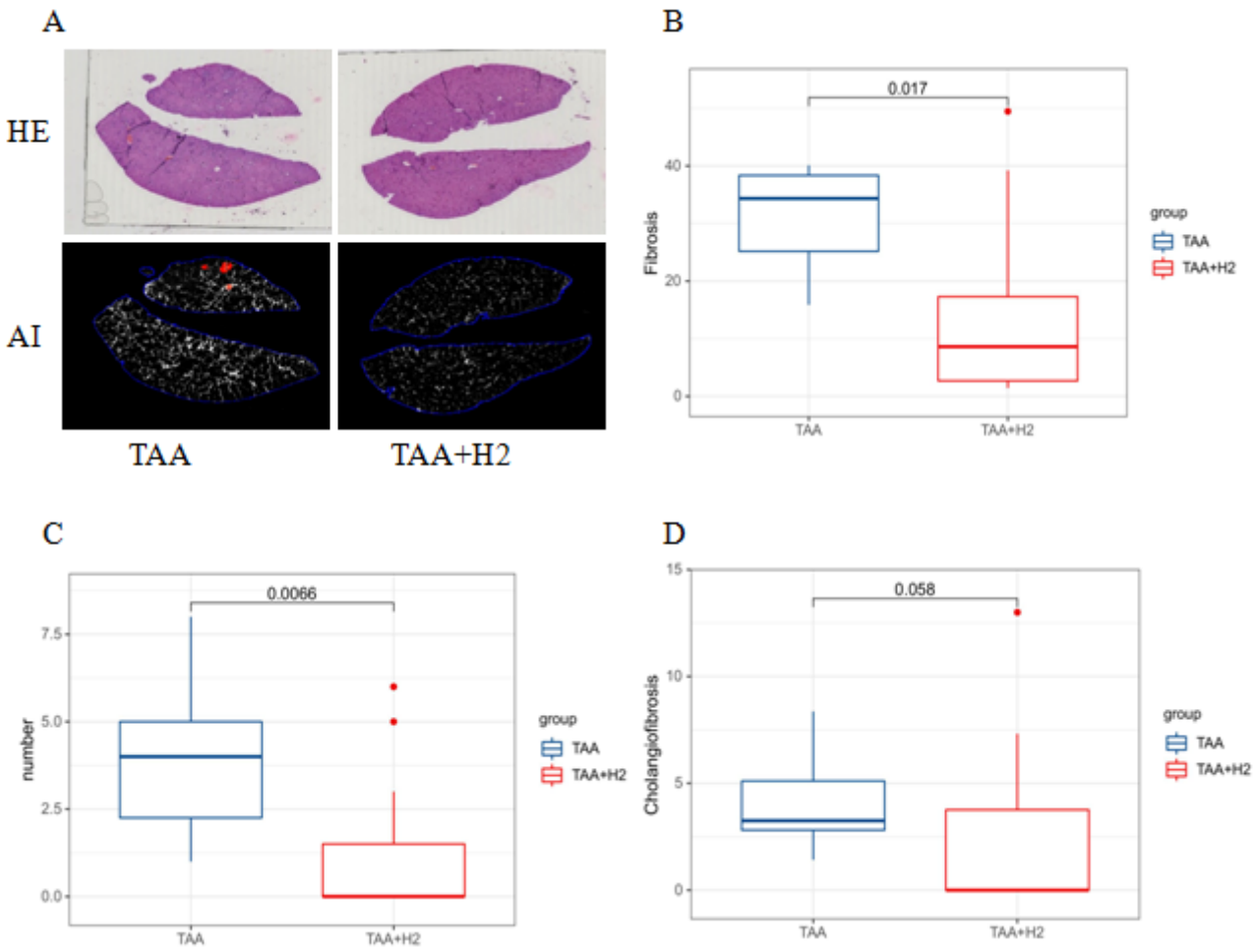


**Figure 5**

**Comparison of AI identification of liver lesions after TAA induction and after TAA+H2 intervention and quantitative analysis.**

A. AI identification of liver histopathology in rats after TAA and TAA+H2 treatment. B. Percentage of liver fibrosis. C. Number of liver tumors. D. Percentage of cholangiofibrosis. T-test was used to determine statistical significance. * $p < 0.05$.

# Supplementary Files

This is a list of supplementary files associated with this preprint. Click to download.

- FigureS1.pptx